Cost Optimal Integration of Flexible Buildings in Congested Distribution Grids

Sarmad Hanif, *Student Member, IEEE,* Tobias Massier, *Member, IEEE,* H. B. Gooi, *Senior Member, IEEE,* Thomas Hamacher, Thomas Reindl.

***Abstract*—Buildings are candidates for providing flexible demand due to their high consumption and inherent thermal inertia. In the future, flexible demand side reserves may also help to relax the expected higher reserve requirements of the grid due to the presence of renewables. However, this flexible demand might be vulnerable to price signals, as simultaneous increase in consumption by multiple buildings due to low (high) energy (reserves) price periods might cause congestion in distribution grids. In order to integrate congestion free energy and reserve provision from buildings, this paper presents two benchmark pricing methodologies: (1) distribution locational marginal prices (DLMP) and (2) iterative DLMP (iDLMP). Both methods deploy convex optimization to obtain an optimal solution of the original problem. Using dual decomposition, a settlement scheme, which efficiently distributes the congestion cost among involved participants is also presented. Case studies are performed on a benchmark distribution system along with the National Energy Market Singapore's (NEMS) price framework. The results prove that both methods optimally remove congestion from distribution grids and have potential to be integrated into the theoretical framework of liberalized markets. Furthermore, as a comparison, it is shown that the DLMP based prices out performs existing pricing structures of the distribution grid. Hence, using this scheme, the DSO can evaluate existing tariffs and introduce incentives for price responsive demands. However, to support these methods, the high requirement for information sharing in the DLMP method and/or communication technology infrastructure for calculating iDLMPs must exist in the future grid.**

***Index Terms*—Flexible Demand, Buildings, Congestion Management, Convex Optimization, Distribution Grid.**

I. Introduction

Demand flexibility aims to help power systems become more competitive, economical and reliable [1], [2]. Furthermore, flexible demand has also shown the potential to mitigate the variability of renewable energies [3], [4]. Hence, it is expected in the near future that flexible demand can play an integral role in efficiently decarbonizing the power system.

Buildings' share of the worldwide energy usage is almost 40% [5], with approximately half of it being used in their heating, ventilation and air conditioning (HVAC) systems [6]. An energy intensive nation, such as Singapore, observes electricity consumption shares of 42%, 37% and 15% in its industrial, commercial and residential sector, respectively [7]. Notably in Singapore, due to its hot and humid climate, annual energy consumption from space conditioning of the commercial sector almost amounts to 7 TWh (52% of the total) [8]. Hence in principle, commercial buildings have the potential to become a huge source of flexibility [9]. Especially, with the support of their thermal inertia, the temperature is allowed to change slowly even when the power consumption is changed rapidly [10].

However, as pointed out in [11]–[13], there are many challenges which exist for integrating flexibility from commercial buildings into the power system. Among many, the two most important challenges exist in the form of (1) obtaining reliable and controllable building models and (2) providing a smooth framework to achieve a high consensus between the power system and the building operation. Moreover, this integration should be performed considering practical constraints such as the requirement of additional communication technology infrastructure.

A great deal of work had been dedicated for developing building simulation tools [14]. These building models provide understanding of building operations as well as annual/monthly/weekly energy consumption. For obtaining quantifiable demand response (DR) potential of commercial buildings, control-oriented building models were investigated in [15]–[17]. Using these models, flexibility of buildings was exploited to obtain energy efficient and cost optimal operation [18]–[21]. Furthermore, in [22]–[26], the authors also demonstrated power system regulation/reserve services from these building models. It was shown that the inclusion of demand-side reserves could help to improve the operational cost and reliability of the grid. Furthermore, the associated monetary incentives from the reserve provision might be instrumental to motivate aggregators/users to participate in load management programs.

Moving towards integration of a more general flexible demand in power systems, the authors in [27], [28], presented various formulations for integrating price-responsive demand into the transmission grid. A similar approach, but more inclined towards the decentralized demand dispatch, was presented in [29]. Based on dual decomposition, the paper formulated a day-ahead and real-time price-based decentralized coordination algorithm between users/aggregators and system operator. It was motivated that the global Lagrange multipliers (LM) provide a direct interpretation of extra system cost as a response to the overall energy balance constraint.

Even though [27]–[29] focused on transmission grids, but physically, the electricity demand originates from distribution grids. It was shown in [30] that the introduction of price-responsive demand in distribution grids raises local congestion issues. Due to the introduction of electric vehicles (EVs), the authors in [30] presented a comparison of various congestion management techniques in distribution grids. The presented methods in [30] were not exposed to a realistic distribution

grid setting. Hence, questions such as the cost of congestion alleviation and grid utilization among multiple load aggregators under a realistic distribution grid were still left unsettled.

Motivated by the development of dynamic tariffs for alleviating distribution grid congestion [31], in [32], the authors presented linear programming based distribution locational marginal prices (DLMPs). In principle, the method was based on finding LMs of the congestion constraints instead of solving a difficult bi-level problem of [30]. However in [33], it was shown that due to the linear formulation the obtained congestion alleviating solution degenerates. As a remedy, a quadratic programming (QP) based method for calculating DLMPs was presented in [33]. Compared to other congestion alleviation methods [30], the advantages of the DLMP method were: (1) it provided the lowest possible theoretical cost to alleviate congestion and (2) it was easy to realize due to its similarity to the existing locational marginal pricing (LMP) concept. Apart from alleviating congestion, DLMPs were also shown to improve the operation of distributed energy resources in distribution grids [34], [35]. It was shown that by using DLMPs as a price-based control signal, customers' energy efficiency and distribution grid's operation capability could be improved.

We believe that one drawback for calculating globally optimal congestion alleviating DLMPs (as proposed in [33]) is the large amount of data needed by the distribution system operator (DSO). This might raise concerns from aggregators/users regarding their data security and privacy. Furthermore, the presence of large number of loads with varying dynamics in distribution grids may increase the complexity of the DSO optimization problem. Hence, this paper provides an approach for obtaining DLMPs in an independent and decentralized manner. It also extends the analysis of global DLMPs [33] by interpreting them as a tool for improving economic efficiency of the distribution grid. Furthermore, the state-of-the-art literature [31]–[33] concerning congestion alleviation using DLMPs is inclined towards EVs. As explained above, commercial buildings have a huge potential for providing flexibility to the grid. Hence, this paper also presents a building integration aspect in a price-based control framework of distribution grids.

Similar to our concern regarding the theoretical development of DLMPs, demand bids were used in [36]–[38] to remove the need for the DSO to accurately predict energy requirements of its underlying loads. These practical case studies mainly focused on achieving a real-time market-based control of distribution grids. Among many objectives, one of the key focuses of these projects was to manage constrained feeders in the distribution grid. Results from [36], [37] demonstrated that a real-time pricing signal (every 5 minutes) was able to remove congestion in the distribution grid. Authors in [38] proposed a multi-agent system for this market-based control. Furthermore, it was also argued that a multi-agent system provides competence, autonomy and equilibrium to the whole system.

This paper also recognizes the importance of a market-based framework for integrating flexible commercial buildings into the distribution grid. In addition, the presented distributed variant of DLMPs of this paper connects the theoretically optimal congestion removal [33] with practically relevant case studies [36]–[38]. Hence, the presented methods in this paper remain practically relevant, while providing a validation framework for integrating congestion free flexible demand in the distribution grid. The main contributions of this paper are threefold. First, this paper provides a distributed variant for obtaining (globally) optimal DLMPs. As explained above, this formulation brings the procedure for obtaining theoretical DLMPs in alignment with the currently available communication and infrastructure technology. Second, this paper demonstrates the applicability of the state-of-the-art controllable building models to be used in a combined energy and reserves procurement while respecting distribution grid constraints. Third, using dual decomposition, the essential question of "who pays what", is answered by presenting an economically fair settlement scheme to settle the congestion cost among interested participants of the distribution grid. Furthermore, this settlement is shown to improve economic efficiency of the distribution grid in the presence of price-responsive demand.

This paper substantially extends the previous work of the authors in [39]. The main extensions are in the form of (1) addressing practical applicability of building models to be used in congestion alleviating frameworks of distribution grids, (2) developing a cooperative framework between the DSO and building operation and (3) performing integration of the combined reserve and energy procurement framework into the distribution grid.

The modeling procedure for this paper is explained in Section II. The formulation of congestion alleviation methods and their settlement scheme are presented in Section III. In Section IV, the simulation setup and the obtained results are provided. Section V presents practical implications and compatibility of both methods with the existing literature. The conclusion and future works related to this paper are presented in Section VI.

II. Preliminaries

Notations

For aggregator i at discrete time step k:

$\hat{\mathbf{d}}_{i,k} \in \mathbb{R}^{n_{d,i}}$	External and Internal Disturbances
$\mathbf{p}_{i,k} \in \mathbb{R}^{n_{p,i}}$	Input schedule ($[\mathbf{u}_{i,k}; \mathbf{r}_{i,k}]$)
$\mathbf{x}_{i,k} \in \mathbb{R}^{n_{x,i}}$	Thermal states
$n_{b,i}$, n_f, n_r	Number of buildings, floors and rooms
$n_{x,i}$, $n_{d,i}$, $n_{p,i}$	Number of states ($n_{b,i}{\cdot}n_f{\cdot}n_r{\cdot}n$), disturbances ($n_{b,i}{\cdot}n_f{\cdot}n_r{\cdot}n_{i_d}$) and inputs ($n_{b,i}{\cdot}n_f n_r{\cdot}n_{i_u}{\cdot}n_{i_r}$)

For each zone at time step t (discrete k):

$\hat{d}_t \in \mathbb{R}^{n_{i_d}}$	External and internal disturbances
n, n_{i_u}, n_{i_d}	Number of states, HVACs and disturbances
$p_{\text{heat},t}$, $p_{\text{fan},t}$	Heating and fan power [kW]

$p_k \in \mathbb{R}^{n_{i_r} n_{i_u}}$	Input schedule ([$u_{\mathrm{m},k}$ $r_{\mathrm{m},k}$]') [kg/sec]
$r_{\mathrm{m},k} \in \mathbb{R}^{n_{i_r}}$	HVAC's mass flow reserve schedule [kg/sec]
$u_{m,t} \in \mathbb{R}^{n_{i_u}}$	HVAC's mass flow energy schedule [kg/sec]
$x_t \in \mathbb{R}^n$	Thermal state vector [deg C]

For modeling R-C thermal network:

ρ, Δp, c_{p}	Density of air, pressure difference across the fan, and specific heat capacity of air
τ^i_{ri}, α_{wi}	Transmittance of window i and absorptivity coefficient of wall, respectively
A^i_{ri}, A_{wi}	Total area of window i and total area of the wall wi, respectively
C_{wi}, C_{ri}	Thermal capacitance of wall and room
N_{wi}, N_{ri}	The set of all connected nodes to walls and the room, respectively
$q''_{rad_{ri}}$, $\dot{q}_{int_{ri}}$	Solar radiation and internal heat generation in the room, respectively
r_i	Equal to 0 for internal and 1 for peripheral walls.
R_{ij}	Thermal resistance between node i and j
T_{wi}, T_{ri}, T_{si}	Temperature of walls, rooms and HVAC's supply
wi, ri	number of walls and rooms

For modeling market:

β	Price sensitivity coefficient [Singapore Dollar (SGD)/(kWh)^2]
$c_{0,k}$	Baseline price [SGD/kWh]
z_k	Reserve price [SGD/kWh]

A. Market Model

A liberalized market setting of the NEMS [40] is adopted in this paper. In NEMS, the loads are allowed to bid for reserves and energy provision through the interruptible load (IL) [41] and the DR [42] program, respectively. For every 30-minute time interval, the NEMS publishes the energy and reserve price through the market clearing engine (MCE) of the Energy Market Company (EMC) [43]. General applicability of commercial buildings, participating in IL and DR program is also provided in [39].

1) Energy Price: In this paper, a price modeling procedure similar to [30], [33] is adopted. It is assumed that the wholesale energy price is coupled with the demand. In particular, it means that the net demand (the actual system demand minus the renewables in the grid) is directly correlated with the energy price as:

$$y_k = c_{0,k} + \beta p_k \tag{1}$$

In (1), the demand p_k is correlated with the spot price y_k, through a sensitivity coefficient β. The price corresponding to the base demand is $c_{0,k}$. The procedure for obtaining values of β and $c_{0,k}$ is explained in [30]. The significance of representing the energy price as in (1) is to model the optimization problem as a QP and avoid unrealistic high peaks in the procured demand [30].

2) Reserve Price: To represent reserve services, interruptible load (IL) from buildings is considered. Under the IL program, if the load bid is accepted and called upon, the load operator must curtail its load. The loads are not paid based on the activation, rather on the availability and their presence in the respective reserve groups. In [43], generators are placed in reserves groups. These groups represent their member's response time and output quality. Due to their thermal inertia, buildings are able to vary their power consumption rapidly. Hence, maximum reserve prices z_k at each time step k, as published by the EMC, are used to calculate the payment to the aggregator/user. It means that the reserve provision from buildings is assumed to be placed in the highest quality reserve group of the MCE. In [40], it has also been mentioned that loads, compared to generators, possess a natural advantage when providing reserves.

Note that the market structure explained above allows commercial buildings to procure flexible energy and reserves from the spot market. As of now, there has not been any reflection of distribution grid constraints in this spot market. With the advent of price-responsive demand, this absorption effect of distribution grids can jeopardize their operation [30].

B. Building Model

In the existing literature, (1) data driven models [44], [45], (2) high fidelity physical models [14], [46], [47] and (3) resistance-capacitance (R-C) based physical models [15], [16] of buildings are found. Data driven models provide good performance when operated within trained (historical) data sets. Hence, the main drawback of these models exists in the form of high data requirements, covering range of operating and ambient conditions. High fidelity physical building models represent accurate complex thermal interactions within a building. Applications of these models are mainly limited to the estimation of annual, monthly or weekly energy consumption. The main disadvantages of these types of models are their size and complexity. Hence, they cannot be easily incorporated into optimization problems, which is necessary for quantifying load shifting potential.

For buildings, the R-C model is designed to achieve controllability. These types of models attempt to mitigate issues related to data driven and high fidelity models. Even though R-C models represent a simplified form of high fidelity physical models, they still provide accurate enough prediction of important thermal states of the building. Compared to their counterparts, R-C models are computationally tractable. This property has been specially useful in the utilization of control theory in building operations [17], [19], [26], [48]–[50]. Hence in this paper, an R-C based physical model is used to predict thermal states and energy requirements of the building.

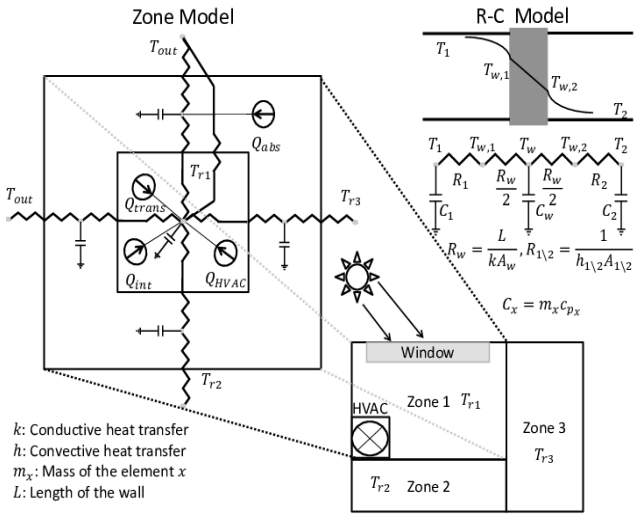

Fig. 1. Simple R-C model representing interpretation of walls and its surrounding environment (top right). The translation of one zone, into an R-C thermal network (left). For simplification, zone 1 is assumed to contain only one room. The injections Q_{HVAC}, Q_{abs} and Q_{int} represent the second, third and fourth term of (2b), respectively. Similarly, Q_{trans} is evaluated using the second term of (2a).

1) Zone Model: An R-C (lumped) model of a zone consists of thermal resistances and thermal capacitances, representing heat transfer and heat storage, respectively. Each node in a zone is represented by one temperature (thermal) state. These nodes are connected with each other through thermal resistances, and to the ground through thermal capacitances. From Fig. 1, it can also be observed that heat flows are represented by current injections, whereas temperatures as voltages. The differential equations representing temperature evolutions of walls and room are:

$$\frac{dT_{wi}}{dt} = \frac{1}{C_{wi}}\left[\sum_{j\in N_{wi}} \frac{T_j - T_{wi}}{R_{ij}} + r_i \alpha_{wi} A_{wi} q''_{rad_{ri}}\right], \quad (2a)$$

$$\frac{dT_{ri}}{dt} = \frac{1}{C_{ri}}\left[\sum_{j\in N_{ri}} \frac{T_j - T_{ri}}{R_{ij}} + \dot{m}_{ri} c_p \left(T_{si} - T_{ri}\right) + w_i \tau^i_{ri} A^i_{ri} q''_{rad_{ri}} + \dot{q}_{int}\right]. \quad (2b)$$

The total number of state equations to represent one zone are $n = wi + ri$. There are two sources of disturbances in the model: (i) external disturbances, experienced due to solar radiation $q''_{rad_{ri}}$ and (ii) internal disturbances, caused by electronic components and occupancy $\dot{q}_{int}$. More details regarding parameters of the R-C model and their units can be found in [15]. From (2), the temperature of the zone x_t can be expressed as a nonlinear combination with the HVAC mass flow rate $u_{\mathrm{m},t}$ as:

$$\dot{x}_t = Ax_t + g(x_t, u_{\mathrm{m},t}) + \hat{d}_t. \quad (3)$$

The expression shown above is of nonlinear nature. Since the most efficient controllers are obtained for linear systems, the nonlinear model described above is linearized and discretized using sequential quadratic programing and zero order hold, respectively [51]. In [51], it is shown that linearizing around the usual operating point does not introduce significant errors. This is mainly because the temperature range of the building is normally not very large. The resultant discrete time linear system at step k becomes:

$$x_{k+1} = Ax_k + B_{\mathrm{u}} u_{\mathrm{m},k} + E\hat{d}_k + B_{\mathrm{r}} r_{\mathrm{m},k},$$
$$x_{k+1} = Ax_k + B_{\mathrm{agg}} p_k + E\hat{d}_k. \quad (4)$$

In (4), p_k represents the augmentation of normal ($u_{\mathrm{m},k}$) and reserve ($r_{\mathrm{m},k}$) consumption variables. Matrices A, B_{agg} and E are of the appropriate sizes. A variable frequency drive fan based HVAC system is considered as a source of flexibility in the modeled zone of each building. In principle, by modulating the fan speed $\dot{m}_{ri}$, the energy consumption as well as the temperature of the room is controlled. Correspondingly, the electrical power consumed for heating $p_{\mathrm{heat},t}$ and fan $p_{\mathrm{fan},t}$ as a function of control variable is given as:

$$p_{\mathrm{heat},t}(u_{\mathrm{m},t}) = \frac{u_{\mathrm{m},t} c_{\mathrm{p}} (T_{si} - T_{ri})}{\eta}, \quad (5a)$$

$$p_{\mathrm{fan},t}(u_{\mathrm{m},t}) = \frac{u_{\mathrm{m},t} \Delta p}{\rho}. \quad (5b)$$

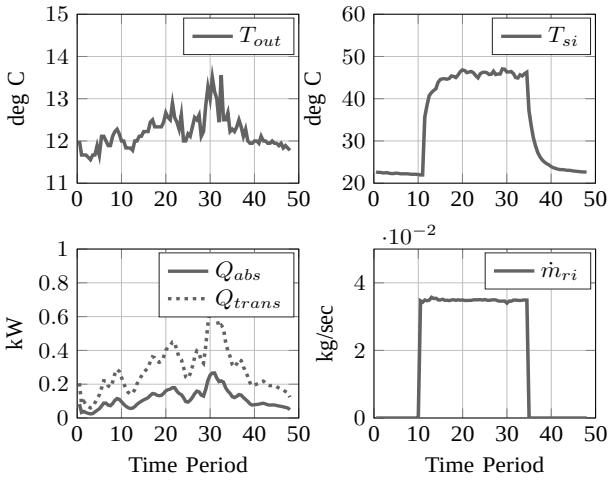

Fig. 2. Measurements used for conducting zone model identification.

2) Identification & Validation: As an initial guess, the R-C thermal model is first developed using typical values of construction materials. In order to adjust the developed theoretical model to represent the actual thermal behavior of the zone, parameters of the model are adjusted. This is performed using the "fmincon" function in Matlab. In particular, optimal parameters are found which minimizes the least square error between the simulated and the actual temperature of the zone. The identified parameters are then used to simulate the thermal behavior of the zone. Figure 3 shows a comparison between the measured temperature of an actual commercial building's zone [15] and the simulated temperature using the identified parameters. The maximum absolute error of only 0.46 deg C is observed in Fig. 3, which has a negligible effect on users. To quantify the performance of the obtained model, two metrics

are defined: (1) the mean absolute percentage error (MAPE) and (2) the mean absolute error (MAE).

$$\text{MAPE} = \frac{1}{N}\sum_{k=1}^{N}\frac{|T_{ri} - T_{mi}|}{T_{mi}} \times 100 \tag{6a}$$

$$\text{MAE} = \frac{1}{N}\sum_{k=1}^{N}|T_{ri} - T_{mi}|. \tag{6b}$$

In (6), T_{mi} and N are the measured temperature of the zone and time duration of the experiment (24 hr), respectively. The MAPE and MAE for the model comes out to be 0.30% and 0.21, respectively. These values show that the modeled temperature evolution is close to the actual one.

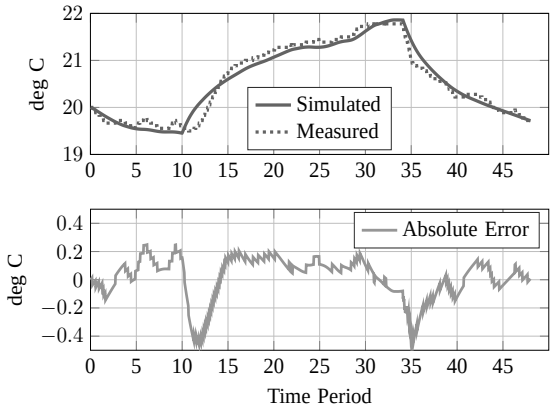

Fig. 3. Comparison between the simulated and actual temperature profile (top), along with the absolute error (bottom).

Similar to the R-C zone network of Fig. 1, the whole building model can also be obtained. Unfortunately, due to the unavailability of data, the validation procedure for a whole building cannot be provided. However, the advantage of physically representing each parameter in R-C models can be used for rapidly translating zone models to the whole building. In Section VII-A, an open source toolbox is deployed to translate an R-C based zone model to the whole building. This translation not only preserves the computational tractability, but it also improves the practical relevance of the adopted modeling approach.

Note that for this paper, deterministic setting, i.e. perfect knowledge of disturbances is assumed. To mitigate disturbance prediction errors, authors in [15] have proposed parameter adaption and error filtering techniques. In principle, these techniques can be included as an additional (real-time) control layer to the overall deterministic framework of buildings and DLMPs. As mitigating the disturbance prediction error is not the prime focus of the presented research, it is not discussed in this paper.

C. Aggregator Model

The aggregator is responsible for procuring flexibility for its contracted buildings. The interaction of the aggregator with its underlying loads and market is shown in Fig. 4. The aggregator i, based on n_r zones in n_f floors of $n_{b,i}$

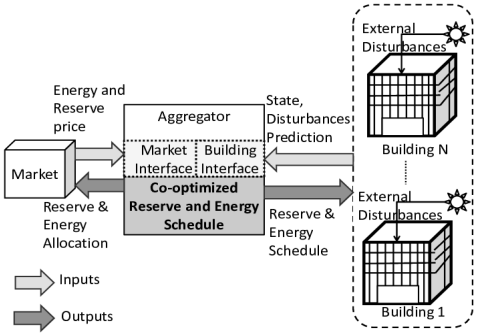

Fig. 4. The Dark grey box represents the objective function of the aggregator. All interfaces have perfect bidirectional communication with no delays and uncertainties.

contracted buildings, augments the zone model of (4) to predict its thermal states as:

$$\mathbf{x}_{i,k} = \mathbf{A}x_{i,0} + \mathbf{B}_{\text{agg}}\mathbf{p}_{i,k} + \mathbf{E}\hat{\mathbf{d}}_{i,k} \tag{7}$$

1) Cost Optimal Energy and Reserve Provision: The cost $J_{\text{sum}_{i,k}}$ for procuring energy by the aggregator i is given as:

$$J_{\text{sum}_{i,k}} = J_{u_{\text{m}_{i,k}}} + J_{r_{\text{m}_{i,k}}} - R_{r_{\text{m}_{i,k}}} \tag{8}$$

where $J_{u_{\text{m}_{i,k}}}$ and $J_{r_{\text{m}_{i,k}}}$ are the cost of consumption due to variables $u_{\text{m},k}$ and $r_{\text{m},k}$, respectively. $R_{r_{\text{m}_{i,k}}}$ represents the revenue due to the allocation of reserves. Using (1), the cost for a constant time interval Δt becomes:

$$\begin{aligned} J_{u_{\text{m}_{i,k}}} &= y_k p(u_{\text{m},k})\Delta t, \\ J_{u_{\text{m}_{i,k}}} &= c_{0,k}p(u_{\text{m},k})\Delta t + \beta(p(u_{\text{m},k})\Delta t)^2 \end{aligned} \tag{9}$$

where $p(u_{\text{m},k}) = p_{\text{heat},k}(u_{\text{m},k}) + p_{\text{fan},k}(u_{\text{m},k})$. Similarly, the cost and revenue from the allocation of reserves are written as:

$$J_{r_{\text{m}_{i,k}}} = c_{0,k}p(r_{\text{m},k})\Delta t + \beta(p(r_{\text{m},k})\Delta t)^2 \tag{10}$$

$$R_{r_{\text{m}_{i,k}}} = z_k p(r_{\text{m},k})\Delta t \tag{11}$$

Substituting (9) – (11) in (8), the total cost takes the quadratic form as:

$$J_{sum_k} = c_k^T p_k + \frac{1}{2}p_k^T B p_k \tag{12}$$

with,

$$c_k = \begin{bmatrix} c_{0,k} \\ c_{0,k} - z_k \end{bmatrix}, \; B = \begin{bmatrix} \beta & 0 \\ 0 & \beta \end{bmatrix} \tag{13}$$

And to allow for the ease of representing the cost function, $p_k = p_k \Delta t$ is assumed. For aggregator i, the total cost at time step k becomes:

$$\mathbf{J}_{sum_{i,k}} = \mathbf{c}_k^{\mathbf{T}}\mathbf{p}_{i,k} + \frac{1}{2}\mathbf{p}_{i,k}^{\mathbf{T}}\mathbf{B}\mathbf{p}_{i,k} \tag{14}$$

Here, $\mathbf{c}_k \in \mathbb{R}^{n_{p,i}}$ and $\mathbf{B} \in \mathbb{R}^{n_{p,i} \times n_{p,i}}$ are the augmented and block diagonal versions of c_k and B, respectively. For the

cost function defined in (13), the optimization problem for aggregator i and time duration N_t is:

$$\min_{\mathbf{p}^*_{i,k}} \sum_{k\in N_t} \mathbf{J}_{sum_{i,k}} \tag{15a}$$

subject to

$$\mathbf{x}^c_{i,k+1} = \mathbf{A}\mathbf{x}^{nc}_{i,k} + \mathbf{B}^c_{\text{agg}}\mathbf{p}_{i,k} + \mathbf{E}\hat{\mathbf{d}}_{i,k} \tag{15b}$$

$$\mathbf{x}^{nc}_{i,k+1} = \mathbf{A}\mathbf{x}^{nc}_{i,k} + \mathbf{B}^{nc}_{\text{agg}}\mathbf{p}_{i,k} + \mathbf{E}\hat{\mathbf{d}}_{i,k} \tag{15c}$$

$$\mathbf{x}^{min}_{i,k} \le \mathbf{x}^c_{i,k} \le \mathbf{x}^{max}_{i,k} \tag{15d}$$

$$\mathbf{x}^{min}_{i,k} \le \mathbf{x}^{nc}_{i,k} \le \mathbf{x}^{max}_{i,k} \tag{15e}$$

$$\mathbf{u}^{min}_{i,k} \le \mathbf{A}^{\text{sum}}\mathbf{p}_{i,k} \le \mathbf{u}^{max}_{i,k} \tag{15f}$$

$$\mathbf{p}_{i,k}, \mathbf{A}^{\text{diff}}\mathbf{p}_{i,k} \ge \mathbf{0} \qquad \forall k \in N_t \tag{15g}$$

From (15), the aggregator obtains the optimal input $\mathbf{p}^*_{i,k}$ sequence for all contracted buildings. In this context, optimality is in terms of minimizing the total cost of the system. Using (15f) and (15g), the aggregator constrains the actuator limits of all HVAC systems. Matrices $\mathbf{A}^{\text{sum}}$ and $\mathbf{A}^{\text{diff}}$ ($\in \mathbb{R}^{n_b \cdot n_{br} \cdot n_{i_u} \times n_{p,i}}$) contain entries $[1\ \ 1]$ and $[1\ \ -1]$ at the appropriate entries to compactly represent addition and subtraction of $u_{\text{m},k}$ and $r_{\text{m},k}$ variables of each zone. Due to the consideration of reserves, two state trajectories, one for the curtailed (15b) and the other for the non-curtailed (15c) case are always kept feasible using (15d) and (15e), respectively. $\mathbf{B}^{nc}_{\text{agg}}$ and $\mathbf{B}^{c}_{\text{agg}}$ are the not-curtailed and curtailed version of $\mathbf{B}_{\text{agg}}$, respectively.

The aggregator formulation does not consider any minimum/maximum energy purchase outside the underlying loads. This condition can be modeled by modifying bounds on the input schedule. Other preferences such as conditional value at risk under price uncertainties can also be formulated as linear constraints [29], [52]. Hence, these variations of the original formulation would still conserve the convexity of the system. Nevertheless, the compatibility of various aggregator problems within the congestion management framework may also form as an interesting future work.

III. Congestion Alleviation Methods for Optimal Energy and Reserve Provision from Buildings

This section presents two variations for calculating DLMPs. Fig. 5 shows the pictorial representation of the coordination between the DSO and aggregators for both methods.

A. Conventional DLMPs (Method A)

The modified DLMP method for the provision of unified energy and reserve provision from buildings is described as:

1) Using (15), each aggregator submits its optimal consumption and reserve schedule to the DSO.
2) The DSO collects information from the aggregators, network and market and generates an optimal price (DLMPs) to alleviate the congestion.
3) After obtaining DLMPs, the final energy and reserve schedule is calculated by each aggregator and submitted to the market/DSO.

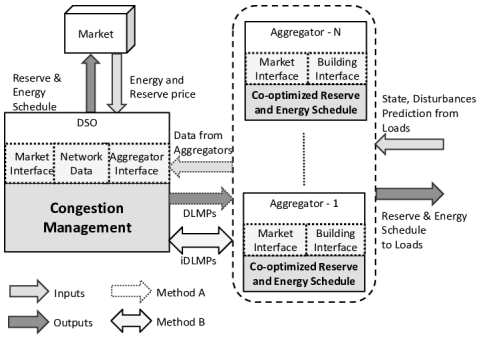

Fig. 5. The coordination between the DSO and the aggregators for calculating DLMPs for both methods. The DSO's interfaces holds similar explanation to the one explained in Fig. 4 for aggregator.

1) DSO Optimization Formulation: For total time N_t and N_i aggregators, the DSO formulates its problem as:

$$\min_{\mathbf{p}^*_{i,k}} \sum_{i\in N_i}\sum_{k\in N_t} \mathbf{J}_{sum_{i,k}} \tag{16a}$$

subject to

$$-f_l \le \sum_{i\in N_i}\sum_{k\in N_t} DM_i\mathbf{p}_{i,k} \le f_l \tag{16b}$$

$$(15\text{b}) - (15\text{g}) \qquad \forall k \in N_t, \forall i \in N_i$$

In (16), the DSO optimizes the total cost of the energy procurement (16a) and constrains each aggregator [(15b) - (15g)] and distribution grid [(16b)] to their operating limits. For distribution grid containing n_{LP} load points (LPs) and n_l distribution lines, matrices $D \in \mathbb{R}^{n_l \times n_{LP}}$ and $M_i \in \mathbb{R}^{n_{LP} \times n_{p,i}}$ represent the power transfer distribution factor and the aggregator i's demand to LPs mapping, respectively. It can be observed that the LMs $\lambda^{+,-}_k (\lambda^+_k - \lambda^-_k, \in \mathbb{R}^{n_l})$ associated with (16b) are only non-zero for the case of line limit violation $f_l \in \mathbb{R}^{n_l}$. Note that line limits in the DSO formulation already account for inflexible demand. Since these loads cannot be procured in the market, they are not included in the objective function of the DSO problem.

2) Modified Aggregator Optimization Formulation: Based on the above mentiond LMs, DLMPs ($\lambda_{\text{dlmp}_{i,k}} = M_i^T D^T \lambda^{+,-}_k + \mathbf{c}$) are formed by the DSO and passed to aggregators. Aggregator i then forms the problem as:

$$\min_{\mathbf{p}^*_{i,k}} \sum_{k\in N_t} \lambda^T_{\text{dlmp}_{i,k}}\mathbf{p}_{i,k} + \frac{1}{2}\mathbf{p}^{\mathbf{T}}_{\text{i},k}\mathbf{B}\mathbf{p}_{\text{i},k} \tag{17}$$

subject to

$$(15\text{b}) - (15\text{g}) \qquad \forall k \in N_t$$

Due to QP formulation, the obtained DLMPs converge to the global optimum [33]. For the case of this paper, i.e. procuring unified energy and reserves from buildings, the proof of the unique solution of the combined aggregator and the DSO problem is presented in Section VII-B.

B. Iterative DLMPs (Method B)

From Fig. 5, it can be seen that in this method, data transfer requirement is replaced by the iterative procedure for

calculating DLMPs i.e. iDLMPs. This decomposition is made possible because, in (16), the only coupling constraint is (16b). To prove this, consider the Lagrange function of (16):

$$
\begin{aligned}
&L(\mathbf{p}_{i,k}, \lambda_k^+, \lambda_k^-, \nu_{i,k}^c, \nu_{i,k}^{nc}, \mu_{i,k}^{+\text{sum}}, \mu_{i,k}^{-\text{sum}}, \mu_{i,k}^{\text{diff}}, \mu_{i,k}^{\mathbf{p}_{i,k}}) = \\
&\sum_{i \in N_i} \sum_{k \in N_t} \mathbf{J}_{sum_{i,k}} + ((\lambda_k^+ - \lambda_k^-)^T (DM_i \mathbf{p}_{i,k} - f_l)) \\
&+ \nu_{i,k}^{c^T} (-\mathbf{x}_{i,k+1}^c + \mathbf{A}\mathbf{x}_{i,k}^{nc} + \mathbf{B}_{\text{agg}}^c \mathbf{p}_{i,k} + \mathbf{E}\hat{\mathbf{d}}_{i,k}) \\
&+ \nu_{i,k}^{nc^T} (\mathbf{x}_{i,k+1}^{nc} - \mathbf{A}\mathbf{x}_{i,k}^{nc} + \mathbf{B}_{\text{agg}}^{nc} \mathbf{p}_{i,k} + \mathbf{E}\hat{\mathbf{d}}_{i,k}) \\
&+ \mu_{i,k}^{+\text{sum}^T} (\mathbf{A}^{\text{sum}} \mathbf{p}_{i,k} - \mathbf{u}_{i,k}^{max}) - \mu_{i,k}^{\mathbf{p}_{i,k}^T} \mathbf{p}_{i,k} \\
&+ \mu_{i,k}^{-\text{sum}^T} (-\mathbf{A}^{\text{sum}} \mathbf{p}_{i,k} + \mathbf{u}_{i,k}^{min}) - \mu_{i,k}^{\text{diff}^T} \mathbf{A}^{\text{diff}} \mathbf{p}_{i,k} \qquad (18)
\end{aligned}
$$

To keep the formulation compact in (18), LMs which are only connected to the input vector are considered. In (18), it is evident that all aggregator's equality ($\nu_{i,k}^c$, $\nu_{i,k}^{nc} \in \mathbb{R}^{n_{x,i}}$) and inequality ($\mu_{i,k}^{+\text{sum}}$, $\mu_{i,k}^{-\text{sum}}$, $\mu_{i,k}^{\text{diff}}$, $\mu_{i,k}^{\mathbf{p}_{i,k}} \in \mathbb{R}^{n_{p,i}}$) LMs are local, except the ones connected to constraint (16b) i.e. $\lambda_k^{+,-}$. In the literature, these problems can be decomposed very efficiently through dual decomposition [53]. In this method, the master (DSO) problem is decomposed into i independent subproblems (aggregators). The global LM are then updated using the projected subgradient/gradient algorithm.[1]

1) Subgradient Algorithm: Consider the partial Lagrangian of the DSO problem with the global LMs and the objective function:

$$
L(\mathbf{p}_{i,k}, \lambda_k^{+,-}) = \sum_{k \in N_t} \mathbf{J}_{sum_{i,k}} + \lambda_k^{+,-^T} (DM_i \mathbf{p}_{i,k} - f_l). \quad (19)
$$

The dual of the above partial Lagrangian is given as:

$$
\begin{aligned}
&g(\lambda_k^{+,-}) = \inf_{\mathbf{p}_{i,k}} L(\mathbf{p}_{i,k}, \lambda_k^{+,-}) \\
&= -\lambda_k^{+,-^T} f_l + \inf_{\mathbf{p}_{i,k}} \sum_{k \in N_t} \mathbf{J}_{sum_{i,k}} + \lambda_k^{+,-^T} (DM_i \mathbf{p}_{i,k}). \quad (20)
\end{aligned}
$$

The sub-gradient S_k of the negative of the dual $\partial(-g)(\lambda_k^{+,-}) \in \mathbb{R}^{n_l}$ is then defined as:

$$
S_k = \sum_{k \in N_t} (DM_i \mathbf{p}_{i,k}^*) - f_l. \qquad (21)
$$

With $\mathbf{p}_{i,k}^*$ is obtained after solving the following problem:

$$
\begin{aligned}
&\min_{\mathbf{p}_{i,k}^*} \sum_{k \in N_t} \lambda_{\text{idlmp}_{i,k}}^T \mathbf{p}_{i,k} + \frac{1}{2} \mathbf{p}_{i,k}^{\mathbf{T}} \mathbf{B} \mathbf{p}_{i,k} \qquad (22) \\
&\text{subject to} \\
&(15b) - (15g) \qquad \forall k \in N_t.
\end{aligned}
$$

By observation, it can be seen that $\lambda_{\text{idlmp}_{i,k}}$ is similar to $\lambda_{\text{dlmp}_{i,k}}$. The only difference is that in (22), λ_{idlmp} are calculated iteratively using a dual sub-gradient method as:

1) Initialize the global LMs as: $\lambda_k^{+,-^T} \geq \mathbf{0}$, and publish $\lambda_{\text{idlmp}_{i,k}}$ to each aggregator.
2) Repeat
   a) Each aggregator i solves (22) and submits its schedule $\mathbf{p}_{i,k}^*$ to the DSO
   b) The DSO evaluates line limit violations using (21)
   c) The global LMs are updated using the subprojection as $\lambda_{k+1}^{+,-^T} = (\lambda_k^{+,-^T} + \alpha_k S_k)_+$
3) The procedure is terminated based on a predefined convergence criterion such as line loading tolerance or improvement in the global LMs.

Since (20) is differentiable, $\alpha_k \in \mathbb{R}_+$ is chosen as a small positive constant step size to guarantee the convergence [53]. Please note that $\lambda_{\text{idlmp}_{i,k}}$ is calculated based solely on global LMs update. Since no data is shared among aggregators and the DSO, the proposed method is completely decentralized and can be deployed in a fully distributed manner.

C. Settlement:

For the price $\lambda_k^{*+,-}$ and consumption $\mathbf{p}_{i,k}^*$, the total cost of congestion $g(i)_{sum}$ and its components can be written as:

$$
\begin{aligned}
g(i)_{sum} &= g(i)_{sch} + g(i)_{con} - g(i)_{cap} && (23a) \\
g(i)_{sch} &= \sum_{k \in N_t} \mathbf{c}_k^{\mathbf{T}} \mathbf{p}_{i,k}^* + \frac{1}{2} \mathbf{p}^{*\mathbf{T}}_{i,k} \mathbf{B} \mathbf{p}_{i,k}^* && (23b) \\
g(i)_{con} &= \sum_{k \in N_t} (\lambda_k^{*+} - \lambda_k^{*-})^T (DM_i \mathbf{p}_{i,k}^*) && (23c) \\
g(i)_{cap} &= \sum_{k \in N_t} (\lambda_k^{*+} - \lambda_k^{*-})^T f_l (\frac{N_{i,LP}}{N_{t,LP}}) && (23d)
\end{aligned}
$$

where $g(i)_{sch}$ is the cost for purchasing energy from the wholesale market. Based on the ratio of the aggregator's LPs $N_{i,LP}$ to the total aggregator LPs in the network $N_{t,LP}$, the theoretical capacity cost is distributed as $g(i)_{cap}$. The actual aggregator's contribution to congestion is represented by $g(i)_{con}$. This settlement procedure is somewhat similar to the one presented in [54]. The DSO merely acts as a mediator and subsidizes/penalizes aggregators, based on the under/over utilization of the total grid capacity, respectively.

The above presented settlement seems more intuitive from iDLMPs' point of view. For the generated $\lambda_k^{+,-}$ and schedule $\mathbf{p}_{i,k}$, the DSO evaluates the cost of congestion contribution $g(i)_{con}$ and grid capacity $g(i)_{cap}$ for aggregator i. Using S_k, prices are raised or lowered until they reach an equilibrium. The final relative congestion cost $(g(i)_{con} - g(i)_{cap})$ decides whether the aggregator should be charged more/less based on its over/under utilization of the allocated capacity. Using this integrated settlement scheme, competition among aggregators could be created to push for efficiency in their energy consumption. Furthermore, by settling the congestion cost locally within the distribution grid, the presented scheme also decouples transmission grid tariffs from the distribution grid dynamics.

Table I
SIMULATION SETUP

Case	Constrained LPs	α_k	Line limits (kW)	β SGD/(kWh)^2
1	6, 7	0.15	1,200	$1 \cdot 10^{-4}$
2	6, 7, 24, 25	0.25	1,300	$1 \cdot 10^{-4}$

[1]The subgradient becomes a gradient when the objective function is differentiable

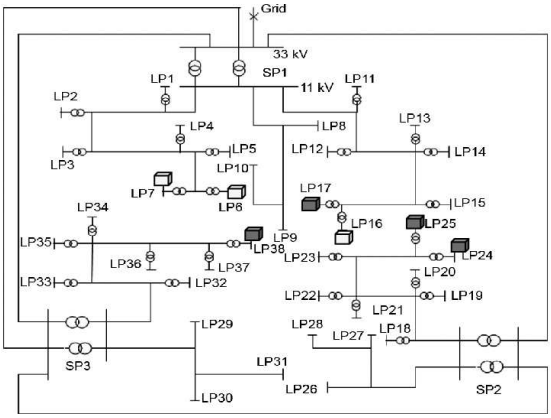

Fig. 6. The modified RBTS distribution network from [55]. Dark and light gray buildings are contracted under the aggregator 1 (LP6, 7, 16) and the aggregator 2 (LP17, 24, 25, 38), respectively.

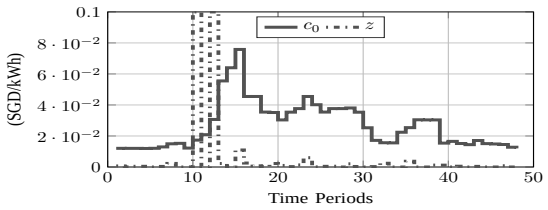

Fig. 7. The energy and reserve price from the EMC Singapore [43] – reserve prices at time step 10 and 12 are synthetically increased to demonstrate the effect of reserve provision on LP's demand. Time period 24 represents exactly the midday.

IV. Simulation Setup and Results

The methods presented above are evaluated on the Bus 4 Distribution Network of Roy Billinton Test System (RBTS) [55]. The performed modifications/assumptions for this paper are presented in Fig. 6. The original network has 7 commercial LPs, with each LP comprising 10 consumers [55]. Each consumer is modeled as a building containing 10 floors and 10 zones. Using this setup, Table I shows the simulated cases of this paper. In Table I, the imposed line limits constrain their respective LPs. To simulate a realistic, but computationally manageable problem under the lack of available data, the measured disturbances (shown in Fig. 2) are taken as a mean value at each step k. The disturbances experienced by each LP are then calculated as normally distributed around that mean value. But no distinction is made in disturbances within one LP. This assumption is in line with the fact that commercial buildings and solar irradiation follow a diurnal pattern. The energy and reserve prices used for conducting simulations are shown in Fig. 7. The optimization problems are formulated in YALMIP [56] and solved using CPLEX [57].

A. Scheduling

For case 1, Fig. 8 represents the response of buildings without the introduction of DLMPs. Even though constraints for buildings are always satisfied, congestion is observed in the distribution grid. The cause of congestion is a combination of high space conditioning requirements, just prior to office hours and attractive reserve provision incentives. For case 1, Fig. 9

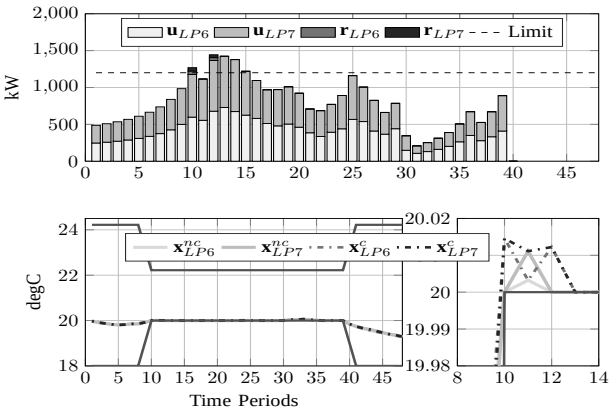

Fig. 8. The cost optimal energy and reserve scheduling for LP6 and LP7 without including DLMPs (top). Feasible temperature trajectories in spite of the curtailing and non-curtailing of reserves (bottom).

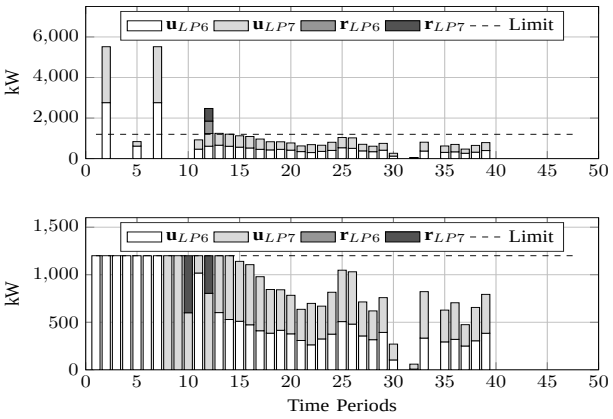

Fig. 9. The aggregator (top) and the DSO (bottom) schedules, due to the deployment of linear programming based DLMPs.

shows the divergence caused by linear programming based DLMPs ($\beta = 0$). It can be observed that the aggregator and the DSO schedule do not converge to the same value, which could make the distribution grid operation inefficient. To avoid issues related to congestion and divergence, QP-based

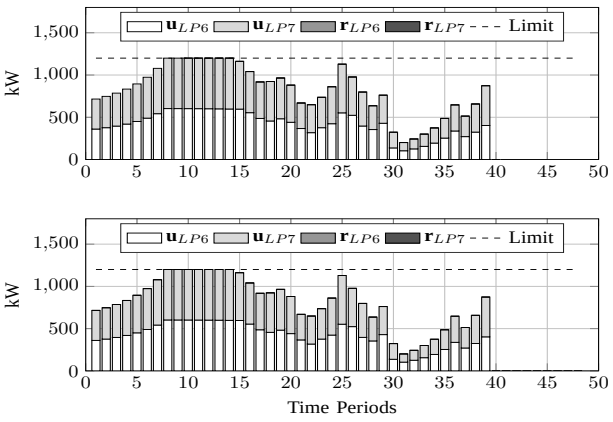

Fig. 10. The congestion free aggregator (top) and the DSO (bottom) schedules, due to the deployment of QP-based DLMPs.

DLMPs are deployed. For case 1, Fig. 10 shows the congestion

Table II
EFFECTIVE DLMPS (SGD/KWH) ($\lambda_{\text{dlmp}} - \mathbf{c}_k$)

Case	LPs	Time						
		8	9	10	11	12	13	14
1	6-7	0.023	0.029	0.046	0.081	0.132	0.203	0.3078
	24-25	0	0	0	0	0	0	0
2	6-7	0	0	0	0.004	0.032	0.071	0.127
	24-25	0	0	0	0	0	0.007	0.044

alleviation after introducing DLMPs. Due to the formulation of strictly convex QPs, both the DSO's and the aggregator's solution converge. This observation is in direct alignment with the theoretical proof presented in Section VII-B. It can be observed that after applying DLMPs, the reserves are not scheduled anymore. This is because the incentives from the reserve provision are outweighed by the introduced DLMPs. Intuitively, it can be said that if reserves are now scheduled at these time periods, they will come at the cost of distribution grid congestion. DLMPs experienced by the constrained LPs for both cases are presented in Table II. Due to the relaxed line loading, in comparison to case 1, DLMPs for case 2 are smaller and fewer than of case 1. In general, as a response to the congestion, the generated DLMPs reflect the load requirement, network constraints and ex-ante market prices.

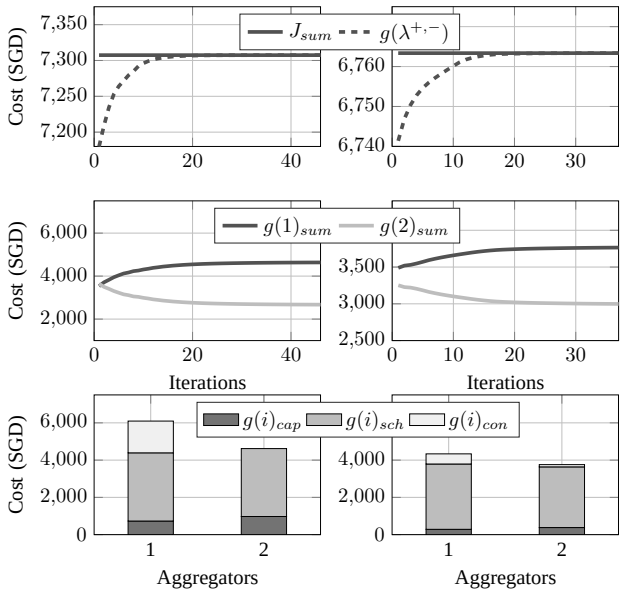

Fig. 11. Convergence of iterative method with the optimal value. Case 1 is plotted on the left and case 2 on the right side.

B. Cost Settlement and iDLMP Performance

The main results from "Method B" are presented in Fig. 11. It can be observed that the final solution of both methods converge to a unique value. Line tolerance of 1×10^{-3} is chosen as the stopping criteria for the subgradient algorithm. Similar results are also obtained for the case of the dual function as the stopping criteria. For both cases, $g(2)_{sum}$ improves at the end of the algorithm. This is because, in comparison to aggregator 1, aggregator 2 has a higher capacity utilization cost ($g(i)_{cap}$) and a lower congestion contribution cost ($g(i)_{con}$). The reason for the high $g(i)_{cap}$ is the larger number of contracted LPs by aggregator 2. $g(i)_{con}$ is observed to be lower due to smaller energy consumption of buildings connected at LP24 and LP25. Aggregator 2 is also not charged for any congestion cost for case 1. This is because none of its LPs are constrained in case 1. To assess iteration requirements

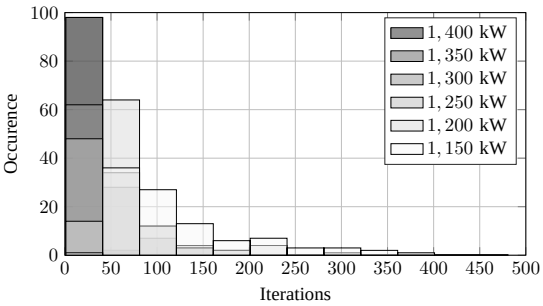

Fig. 12. Number of iterations required to reach the global optimum by the distributed algorithm.

for iDLMPs, the simulation setup is repeated 100 times for various line loading limits. Results from case 1 are presented in Fig. 12. Due to the strictness of limits, an increase in the iteration count is observed. The highest number of iterations (368) is recorded for the line limit of 1,150 kW. Due to strict energy requirements of buildings, the problem gets infeasible for line limits lower than 1,150 kW. Hence, this study can also help both the DSO and the aggregator to evaluate their systems with respect to given load and network requirements. For this paper, the iDLMPs are implemented in a sequentially written program on a 2.4 GHz processor with 64 GB RAM. If the formulation of the aggregator problems is performed offline (5–10s), then each iteration takes 0.05–0.07s. Hence, the worst case (368 iterations) is simulated within 24s, enough for the 30-minute time interval of the NEMS. Of course these values depend on the size and details of the aggregator model. However, since the method is completely distributed, parallel implementation would further decrease the execution time.

C. Economic Efficiency

This section demonstrates the superiority of DLMPs in comparison to the common pricing structures of distribution grids. To simplify the analysis, only energy prices are considered in this section. Furthermore, to show the effectiveness of DLMPs in multiple aggregator settings, only case 2 (see Table I) is presented. The considered three types of prices are: (1) time varying energy prices (λ_{lmp}), (2) flat energy price (λ_{flat} = mean(λ_{lmp})) and (3) the DLMP (λ_{dlmp}). It is assumed that feeder 1 (F1) supplies power to LP6 and LP7, whereas feeder 3 (F3) energizes LP24 and 25).

Figure 13 shows a comparison of imposed prices and the resultant power flow across F1 and F3. From Fig. 13, it is obvious that with respect to adhering to the distribution grid line limits, λ_{dlmp} outperforms all other price structures. As explained before, this is because DLMPs reflect the true behavior of distribution grid constraints. For λ_{lmp} and λ_{flat}, the power flow across feeders deviates from the optimal

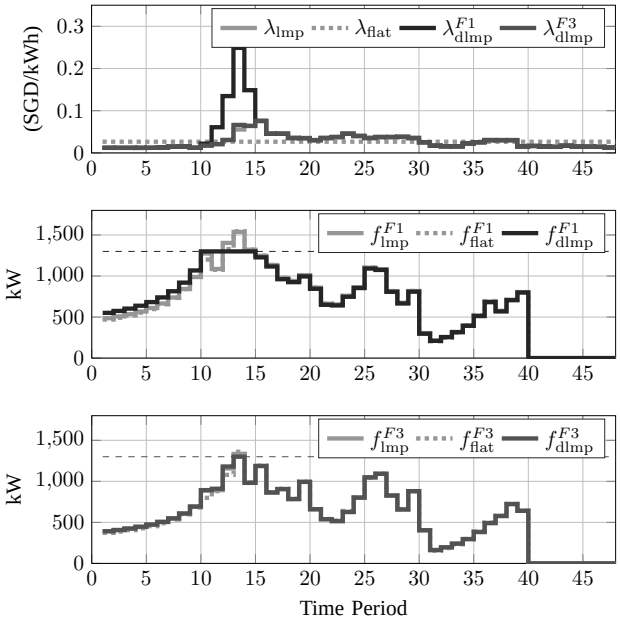

Fig. 13. Prices experienced (top) and the resultant power flow across F1 (middle) and F3 (bottom). Please note λ_{lmp} is similar to c_0 (see Fig. 7).

response. The imposed cost for both aggregators for various prices is presented in Table III. It can be observed that the

Table III
COST (SGD) COMPARISON FOR DIFFERENT TARIFFS

Aggregator	Cost (SGD)	Case		
		λ_{flat}	λ_{lmp}	λ_{dlmp}
1	g_{sch}	$3,510.9$	$3,561.9$	$3,590.8$
	g_{con}	0	0	554.8
	g_{cap}	0	0	243.0
	g_{sum}	$3,510.9$	$3,561.9$	$3,902.6$
2	g_{sch}	$3,516.6$	$3,581.1$	$3,581.3$
	g_{con}	0	0	14.0
	g_{cap}	0	0	325.0
	g_{sum}	$3,516.6$	$3,581.1$	$3,207.3$

usual price structures λ_{lmp} and λ_{flat}, negatively affect the flexibility of demand side resources. In particular, this happens because the cost of congestion is not represented in these prices. Hence, the comparison performed in Table III shows that with the presence of flexible loads in the distribution grid, usual price structures are economically inefficient. For the case of this paper, aggregator 1 is penalized by 8.6% of its original scheduling cost, as it causes more congestion than allowed by the DSO. On the contrary, aggregator 2 is subsidized by approx. 10.4%, due to its underutilization of the grid capacity.

V. IMPLEMENTATION ASPECTS

The presented methods of this paper connect thermal dynamics of buildings with the market-based control framework of distribution grids. Furthermore, this paper also proposes a new iterative-based market clearing method (iDLMPs) for distribution grids. This section highlights the implementation aspect of this paper, compatible with the existing literature. In doing so, this section also gives direction for improving practical realization of the presented methods of this paper.

A. iDLMPs

For iDLMPs, even though the solution is obtained in a completely decentralized manner, the number of exact iterations required to converge to the optimal value are not known in advance (see Fig. 12). Hence, the required IT infrastructure is surely to get overburdened. As a result, some practical consideration must be performed for deploying this method. In [27]–[29], a functional clearing method (demand bids) with a moving horizon (MH) implementation was proposed to solve the iteration problem. The proposed approach used price-based demand functions to efficiently clear the market non-iteratively. Due to linear modeling of buildings, the functional clearing method can also be easily adapted to this paper. Furthermore, as a MH implementation for buildings, authors' previous work [39] showed 30 minutes time step and a MH of 1 day is sufficient for the optimal energy and reserve provision from buildings. In [58], various methods are given to improve the speed of convergence for distributed methods. As convexity of the original formulation is preserved in these methods, iDLMPs can also be efficiently adapted for them.

B. Buildings

The aggregator's prediction of available flexibility in the building is most likely to be communicated through the building management system (BMS), installed in most commercial buildings. Hence, it is imperative that the theoretical building model is compatible to be handled with the current BMS. The authors in [59] discussed a virtual environment in which interaction of buildings, communication networks and power systems was discussed. Similar to Section VII-A, the authors in [59] also used the BRCM toolbox to obtain the reduced order model of the actual building. Furthermore, the authors also presented the necessary communication infrastructure required for operating the DSO and users. For standardizing communication between active participants of DR, opendADR was used [60]. As identified in [59], the work presented in this paper also respects the practical and theoretical constraints. This is because the adopted building model is shown to be easily translatable to BRCM (see Section VII-A), while the presented distributed calculation method requires no data sharing between different entities of the grid.

VI. CONCLUSION & FUTURE WORK

This paper presents two methods for removing congestion in the presence of energy and reserve provision from buildings. By incorporating grid line limits and building energy requirements, an integrated optimal solution is obtained, which respects both network and load constraints, while maximizing the utility of the overall system. Furthermore, using dual decomposition of the original problem, an economically fair settlement scheme for the congestion cost is also presented. The presented methods show high compatibility with the already proposed cost-optimal congestion alleviation strategies in the existing literature. Furthermore, this paper shows the improvement in distribution grid economics, due to the deployment of DLMPs. However, it must be noted that in order to acquire optimal congestion-free energy and reserves

from buildings, availability of high data sharing (DLMPs) or communication infrastructure (iDLMPs) must exist. The future work regarding this paper includes: (1) the computation requirements of DLMPs, and its deviation from the global optimality for the case of uncertainties in prices and energy requirement and losses in the distribution grid, (2) the comparison of demand-bid and iDLMPs and (3) various types of distributed optimization problems to calculate iDLMPs.

VII. Appendix

A. Adapting the R-C Zone Model to BRCM

The main advantages of adopting the BRCM toolbox [61] to generate building models are: (1) it automates the connection of zone differential equation, and (2) it allows for benchmarking and comparing of control/optimization techniques for building simulation [18], [48], [49], [59]. Hence, the zone model described in Section II-B1, is shown to be translatable to BRCM using the description provided below.

The advantage of the BRCM toolbox comes from its ability to separate the dynamic thermal model (heat transfer between rooms, walls etc.) and the static external heat flux (EHF) model (solar and internal gains etc.) of the building. Keeping the similar notation of Section II-B1, the BRCM represents the interaction of thermal states (temperatures), x_t with the aggregated EHF inputs, q_t as:

$$\dot{x}_t = Ax_t + Bq_t(x_t, u_{\mathrm{m},t}, \hat{d}_t). \tag{24}$$

In principle, q_t can be considered as a response in the form of heat due to the influence of control inputs ($u_{\mathrm{m},t}$) and disturbances ($\hat{d}_t$) on the system. For n_u number of inputs, the thermal model in (24) is discretized in order to obtain a bilinear model of the system (the time varying product of states and disturbances with control inputs)[2]

$$\begin{aligned} x_{k+1} &= Ax_k + B_u u_k + E_{\hat{d}}\hat{d}_k \\ &\quad + \sum_{i=1}^{n_u}(E_{\hat{d}u,i}\hat{d}_k + B_{xu,i}x_k)u_{k,i}, \end{aligned} \tag{25}$$

In order to bring the model of (25) into the presented zone model in Section II-B1, two simplifications can be performed: (1) it is assumed that the temperature experienced by the outside of the walls, solar irradiation and heat gains are known in advance (from historical data), and (2) only the HVAC's mass flow is taken as a control input. Under these assumptions, the input dependent state B_{xu} and disturbance $E_{\hat{d}u,i}$ matrices are concatenated into A and E, respectively. Similarly, the model is also extended to provide IL by introducing a reserve vector r_k. The resultant discrete time linear state space model then becomes:

$$x_{k+1} = Ax_k + B_u(u_k + r_k) + E\hat{d}_k \tag{26}$$

As a validation, Fig. 14 shows the comparison between the simulated zone models and the measured temperature. It can be observed that the BRCM toolbox represents a close similarity to the actual temperature evolution. This validation enforces that the BRCM provides an extensible, yet comprehensive tool for modeling the thermal dynamics of a building.

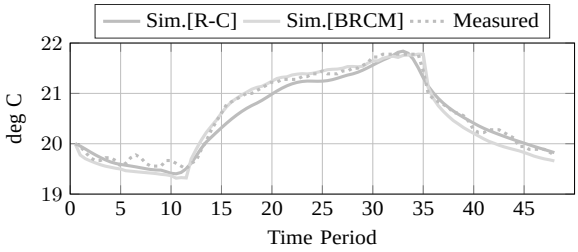

Fig. 14. Temperature profiles of simulated zone models, using BRCM and R-C model(Section II), and their comparison with the actual measurements [15].

B. Proof of Convergence of the DSO and the Aggregator Optimization Problem

The Karush Kuhn Tucker (KKT) conditions for the DSO problem are:

$$\begin{aligned} &\mathbf{c}_k^{\mathbf{T}} + \mathbf{B}\mathbf{p}_{i,k} + M_i^T D^T(\lambda_k^+ - \lambda_k^-) + \mathbf{B}_{\mathrm{agg}}^{c^T}\nu_{i,k}^c + \mathbf{B}_{\mathrm{agg}}^{nc^T}\nu_{i,k}^{nc} \\ &+ \mathbf{A}^{\mathrm{sum}^T}(\mu_{i,k}^{+\mathrm{sum}} - \mu_{i,k}^{-\mathrm{sum}}) - \mathbf{A}^{\mathrm{diff}^T}\mu_{i,k}^{\mathrm{diff}} - \mu_{i,k}^{\mathbf{p}_{i,k}} = 0 \end{aligned} \tag{27}$$

$$\lambda_k^+ \cdot (\sum_{i\in N_i}\sum_{k\in N_t} DM_i\mathbf{p}_{i,k} - f_l) = 0 \tag{28}$$

$$\lambda_k^- \cdot (-\sum_{i\in N_i}\sum_{k\in N_t} DM_i\mathbf{p}_{i,k} - f_l) = 0 \tag{29}$$

$$\mu_{i,k}^{+\mathrm{sum}} \cdot (\mathbf{A}^{\mathrm{sum}}\mathbf{p}_{i,k} - \mathbf{u}_{i,k}^{max}) = 0 \tag{30}$$

$$\mu_{i,k}^{-\mathrm{sum}} \cdot (-\mathbf{A}^{\mathrm{sum}}\mathbf{p}_{i,k} + \mathbf{u}_{i,k}^{min}) = 0 \tag{31}$$

$$\mu_{i,k}^{\mathrm{diff}} \cdot (-\mathbf{A}^{\mathrm{diff}}\mathbf{p}_{i,k}) = 0 \tag{32}$$

$$\mu_{i,k}^{\mathbf{p}_{i,k}} \cdot (-\mathbf{p}_{i,k}) = 0 \tag{33}$$

$$\lambda_k^+, \lambda_k^- \geq 0 \tag{34}$$

$$\mu_{i,k}^{-\mathrm{sum}}, \mu_{i,k}^{+\mathrm{sum}}, \mu_{i,k}^{\mathrm{diff}}, \mu_{i,k}^{\mathbf{p}_{i,k}} \geq 0 \qquad \forall i \in N_i, \forall k \in N_t \tag{35}$$

and [(15b) - (15g)]. Similarly, for the aggregator i problem, the KKT conditions are:

$$\begin{aligned} &\mathbf{c}_k^{\mathbf{T}} + \mathbf{B}\mathbf{p}_{i,k} + M_i^T D^T(\lambda_k^+ - \lambda_k^-) + \mathbf{B}_{\mathrm{agg}}^{c^T}\nu_{i,k}^c + \mathbf{B}_{\mathrm{agg}}^{nc^T}\nu_{i,k}^{nc} \\ &+ \mathbf{A}^{\mathrm{sum}^T}(\mu_{i,k}^{+\mathrm{sum}} - \mu_{i,k}^{-\mathrm{sum}}) - \mathbf{A}^{\mathrm{diff}^T}\mu_{i,k}^{\mathrm{diff}} - \mu_{i,k}^{\mathbf{p}_{i,k}} = 0 \end{aligned} \tag{36}$$

$$\mu_{i,k}^{-\mathrm{sum}} \cdot (\mathbf{A}^{\mathrm{sum}}\mathbf{p}_{i,k} - \mathbf{u}_{i,k}^{max}) = 0 \tag{37}$$

$$\mu_{i,k}^{-\mathrm{sum}} \cdot (-\mathbf{A}^{\mathrm{sum}}\mathbf{p}_{i,k} + \mathbf{u}_{i,k}^{min}) = 0 \tag{38}$$

$$\mu_{i,k}^{\mathrm{diff}} \cdot (-\mathbf{A}^{\mathrm{diff}}\mathbf{p}_{i,k}) = 0 \tag{39}$$

$$\mu_{i,k}^{\mathbf{p}_{i,k}} \cdot (-\mathbf{p}_{i,k}) = 0 \qquad \forall k \in N_t \tag{40}$$

along with [(35), (15b) - (15g)].

By observing the DSO QP, one can see that the Hessian matrix of the quadratic term in the objective function (16a) is a positive definite matrix. Hence, the QP in (16), containing the positive definite matrix in the objective function and affine constraints, is strictly convex. This problem yields a unique minimizer and its KKT conditions are necessary and sufficient [62]. Similar arguments apply to the aggregator's QP.

Since a solution of the KKT condition of the DSO problem, $(\mathbf{p}_{i,k}^*, \mu_{i,k}^{-\mathrm{sum}*}, \mu_{i,k}^{+\mathrm{sum}*}, \mu_{i,k}^{\mathrm{diff}*}, \mu_{i,k}^{\mathbf{p}_{i,k}*}, \nu_{i,k}^{c*}, \nu_{i,k}^{nc*}, \lambda_k^{+*}, \lambda_k^{-*})$, respects DSO problem constraints [(15b) – (15g), (16b)]

[2]Refer to [61] for the more information regarding the thermal model and its corresponding matrices of BRCM.

and its KKT conditions [(27) – (35)]. This implies that a solution ($\mathbf{p}^{*}_{i,k}$) is a solution of the DSO optimization problem. Similarly, the solution of the aggregator i's QP, ($\mathbf{p}^{**}_{i,k}$, $\mu^{-\mathrm{sum}**}_{i,k}$, $\mu^{+\mathrm{sum}**}_{i,k}$, $\mu^{\mathrm{diff}**}_{i,k}$, $\mu^{\mathbf{p}_{i,k}**}_{i,k}$, $\nu^{c*}_{i,k}$, $\nu^{nc**}_{i,k}$) also satisfies its individual constraints [(15b) – (15g)] and KKT conditions [(36) – (40), (35)]. By observation, the DSO problem has all aggregator constraints embeded in it. Hence, $\mathbf{p}^{*}_{i,k}$ is also a valid solution of the aggregator problem. But the solution of the aggregator problem may not be the solution of the DSO's problem, because each aggregator is not responsible for line limits [(28) and (29)]. However, due to the solution of the DSO and aggregator problem being unique, the solution of the aggregator problem must also be a valid solution to the DSO problem ($\mathbf{p}^{*}_{i,k} = \mathbf{p}^{**}_{i,k}$).

REFERENCES

[1] J. Torriti, M. G. Hassan, and M. Leach, "Demand response experience in Europe: Policies, programmes and implementation," *Energy*, vol. 35, no. 4, pp. 1575–1583, 2010.

[2] Federal Energy Regulatory Commission, "Assessment of Demand Response and Advanced Metering," Federal Energy Regulatory Commision, Tech. Rep., 2015. [Online]. Available: http://www.ferc.gov/legal/staff-reports/2015/demand-response.pdf

[3] J. M. Morales, A. J. Conejo, H. Madsen, P. Pinson, and M. Zugno, *Integrating Renewables in Electricity Markets*, ser. International Series in Operations Research & Management Science. Boston, MA: Springer US, 2014, vol. 205.

[4] D. a. Halamay, T. K. a. Brekken, A. Simmons, and S. McArthur, "Reserve Requirement Impacts of Large-Scale Integration of Wind, Solar, and Ocean Wave Power Generation," *IEEE Transactions on Sustainable Energy*, vol. 2, no. 3, pp. 321–328, 2011.

[5] L. Pérez-Lombard, J. Ortiz, and C. Pout, "A review on buildings energy consumption information," *Energy and Buildings*, vol. 40, no. 3, pp. 394–398, Jan. 2008.

[6] "Buildings Energy Data Book." [Online]. Available: http://buildingsdatabook.eren.doe.gov/ChapterIntro1.aspx

[7] EMA, "Singapore Energy Statistics," Energy Market Authority, Singapore, Tech. Rep., 2015. [Online]. Available: http://tinyurl.com/zamtw5p

[8] C. Qi, "Office Building Energy Saving Potential In Singapore," National University of Singapore, Tech. Rep., 2006. [Online]. Available: http://tinyurl.com/h3htlsw

[9] D. Kolokotsa, "The role of smart grids in the building sector," *Energy and Buildings*, vol. 116, pp. 703–708, Mar. 2016. [Online]. Available: http://linkinghub.elsevier.com/retrieve/pii/S0378778815005447

[10] J. E. Braun, "Load Control Using Building Thermal Mass," *Journal of Solar Energy Engineering*, vol. 125, no. 3, p. 292, 2003.

[11] J. Baillieul, M. C. Caramanis, and M. D. Ilic, "Control Challenges in Microgrids and the Role of Energy-Efficient Buildings [Scanning the Issue]," *Proceedings of the IEEE*, vol. 104, no. 4, pp. 692–696, Apr. 2016.

[12] J.-Y. Joo and M. D. Ilic, "An Information Exchange Framework Utilizing Smart Buildings for Efficient Microgrid Operation," *Proceedings of the IEEE*, vol. 104, no. 4, pp. 858–864, Apr. 2016.

[13] T. Samad, E. Koch, and P. Stluka, "Automated Demand Response for Smart Buildings and Microgrids: The State of the Practice and Research Challenges," *Proceedings of the IEEE*, vol. 104, no. 4, pp. 726–744, 2016.

[14] D. B. Crawley, J. W. Hand, M. Kummert, and B. T. Griffith, "Contrasting the capabilities of building energy performance simulation programs," *Building and Environment*, vol. 43, no. 4, pp. 661–673, Apr. 2008.

[15] M. Maasoumy, "Controlling Energy-Efficient Buildings in the Context of Smart Grid: A Cyber Physical System Approach," Ph.D. dissertation, University of California, Berkeley, 2013. [Online]. Available: http://www.eecs.berkeley.edu/Pubs/TechRpts/2013/EECS-2013-244.html

[16] David Sturzenegger, "Model Predictive Building Climate Control - Steps Towards Practice," Ph.D. Thesis, ETH Zurich, 2012. [Online]. Available: http://tinyurl.com/hldpwq7

[17] Y. Ma, A. Kelman, A. Daly, and F. Borrelli, "Predictive Control for Energy Efficient Buildings with Thermal Storage: Modeling, Stimulation, and Experiments," *IEEE Control Systems*, vol. 32, no. 1, pp. 44–64, 2012.

[18] D. Sturzenegger, D. Gyalistras, M. Morari, and R. S. Smith, "Model Predictive Climate Control of a Swiss Office Building: Implementation, Results, and Cost-Benefit Analysis," *IEEE Transactions on Control Systems Technology*, vol. 24, no. 1, pp. 1–12, 2016.

[19] F. Oldewurtel, A. Parisio, C. N. Jones, D. Gyalistras, M. Gwerder, V. Stauch, B. Lehmann, and M. Morari, "Use of model predictive control and weather forecasts for energy efficient building climate control," *Energy and Buildings*, vol. 45, pp. 15–27, Feb. 2012.

[20] Y. Ma, F. Borrelli, B. Hencey, B. Coffey, S. Bengea, and P. Haves, "Model Predictive Control for the Operation of Building Cooling Systems," *IEEE Transactions on Control Systems Technology*, vol. 20, no. 3, pp. 796–803, 2012.

[21] M. Maasoumy and A. Sangiovanni-Vincentelli, "Total and Peak Energy Consumption Minimization of Building HVAC Systems Using Model Predictive Control," *IEEE Design & Test of Computers*, vol. 29, no. 4, pp. 26–35, 2012.

[22] E. Vrettos and G. Andersson, "Scheduling and Provision of Secondary Frequency Reserves by Aggregations of Commercial Buildings," *IEEE Transactions on Sustainable Energy*, vol. 7, no. 2, pp. 850–864, 2016.

[23] E. Vrettos, F. Oldewurtel, and G. Andersson, "Robust Energy-Constrained Frequency Reserves From Aggregations of Commercial Buildings," *IEEE Transactions on Power Systems*, pp. 1–14, 2016.

[24] W. Mai, S. Member, C. Y. Chung, and S. Member, "Economic MPC of Aggregating Commercial Buildings for Providing Flexible Power Reserve," *IEEE Trans. Power Syst.*, vol. 30, no. 5, pp. 2685–2694, 2015.

[25] Y. Lin, P. Barooah, S. Meyn, and T. Middelkoop, "Experimental Evaluation of Frequency Regulation From Commercial Building HVAC Systems," *IEEE Transactions on Smart Grid*, vol. 6, no. 2, pp. 776–783, Mar. 2015.

[26] M. Maasoumy, C. Rosenberg, A. Sangiovanni-Vincentelli, and D. S. Callaway, "Model predictive control approach to online computation of demand-side flexibility of commercial buildings HVAC systems for Supply Following," in *2014 American Control Conference*. IEEE, Jun. 2014, pp. 1082–1089.

[27] M. D. Ilic, L. Xie, and J.-Y. Joo, "Efficient Coordination of Wind Power and Price-Responsive Demand - Part I: Theoretical Foundations," *IEEE Transactions on Power Systems*, vol. 26, no. 4, pp. 1885–1893, 2011.

[28] M. D. Ilic, L. Xie, and J.-y. Joo, "Efficient Coordination of Wind Power and Price-Responsive Demand - Part II: Case Studies," *IEEE Transactions on Power Systems*, vol. 26, no. 4, pp. 1875–1884, Nov. 2011.

[29] Jhi-Young Joo and M. D. Ilic, "Multi-Layered Optimization Of Demand Resources Using Lagrange Dual Decomposition," *IEEE Transactions on Smart Grid*, vol. 4, no. 4, pp. 2081–2088, Dec. 2013.

[30] R. Verzijlbergh, L. J. De Vries, and Z. Lukszo, "Renewable Energy Sources and Responsive Demand. Do We Need Congestion Management in the Distribution Grid?" *IEEE Transactions on Power Systems*, vol. 29, no. 5, pp. 2119–2128, 2014.

[31] N. O'Connell, Q. Wu, J. Østergaard, A. H. Nielsen, S. T. Cha, and Y. Ding, "Day-ahead tariffs for the alleviation of distribution grid congestion from electric vehicles," *Electric Power Systems Research*, vol. 92, pp. 106–114, Nov. 2012.

[32] R. Li, Q. Wu, and S. S. Oren, "Distribution Locational Marginal Pricing for Optimal Electric Vehicle Charging Management," *IEEE Transactions on Power Systems*, vol. 29, no. 1, pp. 203–211, Jan. 2014.

[33] S. Huang, Q. Wu, S. S. Oren, R. Li, and Z. Liu, "Distribution Locational Marginal Pricing Through Quadratic Programming for Congestion Management in Distribution Networks," *IEEE Transactions on Power Systems*, vol. 30, no. 4, pp. 2170–2178, Jul. 2015.

[34] G. T. Heydt, B. H. Chowdhury, M. L. Crow, D. Haughton, B. D. Kiefer, F. Meng, and B. R. Sathyanarayana, "Pricing and control in the next generation power distribution system," *IEEE Transactions on Smart Grid*, vol. 3, no. 2, pp. 907–914, 2012.

[35] F. Meng, D. Haughton, B. Chowdhury, M. L. Crow, and G. T. Heydt, "Distributed Generation and Storage Optimal Control With State Estimation," *IEEE Transactions on Smart Grid*, vol. 4, no. 4, pp. 2266–2273, Dec. 2013.

[36] D. J. Hammerstrom, R. Ambrosio, T. a. Carlon, J. G. Desteese, R. Kajfasz, R. G. Pratt, and D. P. Chassin, "Pacific Northwest GridWise(TM) Testbed Demonstration Projects Part I . Olympic Peninsula Project," Pacific Northwest National Laboratory, Tech. Rep., 2007.

[37] S. E. Widergren, K. Subbarao, J. C. Fuller, D. P. Chassin, A. Somani, M. C. Marinovici, and J. L. Hammerstrom, "AEP Ohio gridSMART demonstration project real-time pricing demonstration analysis," Pacific Northwest National Laboratory, Tech. Rep. February, 2014.

[38] J. K. Kok, C. J. Warmer, and I. G. Kamphuis, "PowerMatcher," in *Proceedings of the fourth international joint conference on Autonomous agents and multiagent systems - AAMAS '05*, vol. 48, no. 3, 2005, p. 75.

[39] S. Hanif, D. Fernando, M. Maasoumy, T. Massier, T. Hamacher, and T. Reindl, "Model predictive control scheme for investigating demand side flexibility in Singapore," in *2015 50th International Universities Power Engineering Conference (UPEC)*, 2015, pp. 1–6.

[40] Energy Market Authority, "Introduction to the National Electricity Market," Energy Market Authority, Singapore, Tech. Rep. October, 2010. [Online]. Available: http://tinyurl.com/j36eagv

[41] S. Swan, "Interruptible load: new partnerships for better energy management," *2005 International Power Engineering Conference*, pp. 888–892 Vol. 2, 2005.

[42] Energy Market Authority, "Implementing Demand Response In The National Electricity Market of Singapore," EMA, Singapore, Tech. Rep., 2013. [Online]. Available: http://tinyurl.com/zw5lmsn

[43] "Energy Market Company Singapore." [Online]. Available: https://www.emcsg.com/

[44] J. L. Mathieu, D. S. Callaway, and S. Kiliccote, "Variability in automated responses of commercial buildings and industrial facilities to dynamic electricity prices," *Energy and Buildings*, vol. 43, no. 12, pp. 3322–3330, 2011.

[45] J. L. Mathieu, P. N. Price, S. Kiliccote, and M. A. Piette, "Quantifying changes in building electricity use, with application to demand response," *IEEE Transactions on Smart Grid*, vol. 2, no. 3, pp. 507–518, 2011.

[46] TRNSYS, "Trnsys 17 - A Transient System Simulation Program," Solar Energy Laboratory, Univ. of Wisconsin-Madison, Tech. Rep., 2013. [Online]. Available: http://sel.me.wisc.edu/trnsys/features/t17_1_updates.pdf

[47] D. B. Crawley, L. K. Lawrie, F. C. Winkelmann, W. F. Buhl, Y. J. Huang, C. O. Pedersen, R. K. Strand, R. J. Liesen, D. E. Fisher, M. J. Witte, and J. Glazer, "EnergyPlus: Creating a new-generation building energy simulation program," *Energy and Buildings*, vol. 33, no. 4, pp. 319–331, 2001.

[48] M. Gwerder, D. Gyalistras, C. Sagerschnig, R. S. Smith, and D. Sturzenegger, "Final Report: Use of Weather And Occupancy Forecasts For Optimal Building Climate Control (OptiControl)," ETH Zürich, Tech. Rep. September, 2010. [Online]. Available: http://www.opticontrol.ethz.ch/Lit/Gyal_10_Rep-OptiCtrlFinalRep.pdf

[49] ——, "Final Report: Use of Weather And Occupancy Forecasts For Optimal Building Climate Control Part II : Demonstration (OptiControl-II)," ETH Zürich, Tech. Rep. September, 2013. [Online]. Available: http://www.opticontrol.ethz.ch/Lit/Gwer_13_Rep-OptiCtrl2FinalRep.pdf

[50] F. Oldewurtel, C. N. Jones, and M. Morari, "A tractable approximation of chance constrained stochastic MPC based on affine disturbance feedback," in *Proceedings of the IEEE Conference on Decision and Control*, 2008, pp. 4731–4736.

[51] M. Maasoumy, A. Pinto, and A. Sangiovanni-Vincentelli, "Model-Based Hierarchical Optimal Control Design for HVAC Systems," in *ASME 2011 Dynamic Systems and Control Conference and Bath/ASME Symposium on Fluid Power and Motion Control, Volume 1*, 2011, pp. 271–278.

[52] S. Sarykalin, G. Serraino, and S. Uryasev, "Value-at-Risk vs . Conditional Value-at-Risk in risk management and optimization," *Tutorials in Operations Research, INFORMS*, pp. 270–294, 2008.

[53] S. Boyd, L. Xiao, A. Mutapcic, and J. Mattingley, "Notes on Decomposition Methods," Stanford University, Tech. Rep., 2008. [Online]. Available: https://see.stanford.edu/materials/lsocoee364b/08-decomposition_notes.pdf

[54] B. Biegel, P. Andersen, J. Stoustrup, and J. Bendtsen, "Congestion management in a smart grid via shadow prices," in *8th IFAC Symposium on Power Plant and Power System Control*, F. Maurice, Ed., Sep. 2012, pp. 518–523.

[55] R. Allan, R. Billinton, I. Sjarief, L. Goel, and K. So, "A reliability test system for educational purposes-basic distribution system data and results," *IEEE Transactions on Power Systems*, vol. 6, no. 2, pp. 813–820, May 1991.

[56] J. Loefberg, "YALMIP: A toolbox for Modeling and Optimization in MATLAB," in *CACSD Conference*, Taipei, 2004.

[57] IBM, "IBM ILOG CPLEX Optimization Studio." [Online]. Available: http://www-03.ibm.com/software/products/en/ibmilogcpleoptistud

[58] S. Boyd, N. Parikh, B. P. E Chu, and J. Eckstein, "Distributed Optimization and Statistical Learning via the Alternating Direction Method of Multipliers," *Foundations and Trends in Machine Learning*, vol. 3, no. 1, pp. 1–122, 2011.

[59] S. Chatzivasileiadis, M. Bonvini, J. Matanza, R. Yin, T. S. Nouidui, E. C. Kara, R. Parmar, D. Lorenzetti, M. Wetter, and S. Kiliccote, "Cyber-physical modeling of distributed resources for distribution system operations," *Proceedings of the IEEE*, vol. 104, no. 4, pp. 789–806, 2016.

[60] "OpenADR Alliance." [Online]. Available: http://www.openadr.org/

[61] D. Sturzenegger, V. Semeraro, D. Gyalistras, and R. S. Smith, "Building Resistance-Capacitance Modeling (BRCM) ToolBox," 2012. [Online]. Available: http://www.brcm.ethz.ch

[62] L. Boyd, Stephen and Vandenberghe, *Convex optimization theory*. Cambridge University Press, 2004.

Sarmad Hanif (S'15) received B.Sc. in Electrical Engineering from the University of Engineering and Technology Lahore, Pakistan and M.Sc. in Power Engineering from the Technical University of Munich (TUM), Germany in 2009 and 2013, respectively. Since June 2014, he is pursuing Ph.D. at the Technical University of Munich (TUM), Germany. He is interested in the integration of cost effective and reliable flexible demand into power systems.

Tobias Massier (M'15) received the Dipl.-Ing. and PhD degree in electrical engineering and information technology from the Technical University of Munich (TUM), Germany, in 2002 and 2010 respectively. From 2009 to 2012, he managed a new Master Program in Power Engineering at TUM. Since 2013, he has been with TUM CREATE as Principal Investigator of the research group Electrification Suite and Test Lab. His research interests are in transportation electrification, vehicle emissions and integration of renewable energies.

H. B. Gooi (SM'95) received the B.S. degree in EE from National Taiwan University in 1978; the M.S. degree in EE from the University of New Brunswick in 1980; and the Ph.D. degree in EE from Ohio State University in 1983. From 1983 to 1985, he was an Assistant Professor with Lafayette College, Easton. From 1985 to 1991, he was a Senior Engineer with Empros (now Siemens), Minneapolis, where he was responsible for the design and testing coordination of domestic and international energy management system projects. In 1991, he joined the School of Electrical and Electronic Engineering, Nanyang Technological University, Singapore, as a Senior Lecturer, where he has been an Associate Professor since 1999. He was the Deputy Head of Power Engineering Division during 2008-2014. He has been an Editor of IEEE Transactions on Power Systems since 2016. His current research interests include microgrid energy management systems dealing with storage, renewable energy sources, electricity market and spinning reserve.

Thomas Hamacher is a full professor in renewable and sustainable energy systems at the Technical University Munich (TUM), Germany. His research focuses on energy and systems analysis, focusing on urban energy systems, the integration of renewable energy into the power grid, and innovative nuclear systems (including fusion). Other focuses of his work are the methods and fundamentals of energy models.

Thomas Reindl is the Deputy CEO of the Solar Energy Research Institute of Singapore (SERIS) and a Principal Research Fellow (equivalent to Associate Professor) at the National University of Singapore (NUS). Before joining SERIS, Dr. Reindl held several management positions within the solar industry. Dr. Reindl holds a Master in Chemistry, a Ph.D. in Natural Sciences and an MBA from INSEAD, all awarded with the highest honours. In addition to his appointment as Deputy CEO of the institute, he is also Director of the Solar Energy Systems cluster at SERIS since 2010.